Characterization of Met25 as a Color Associated Genetic Marker in *Yarrowia lipolytica*

Harley Edwards [1], Zhiliang Yang [1] and Peng Xu [1*]

[1] Department of Chemical, Biochemical and Environmental Engineering, University of Maryland Baltimore County, Baltimore, MD 21250

[*] Corresponding author Tel: +1(410)-455-2474; fax: +1(410)-455-1049.

E-mail address: pengxu@umbc.edu (Peng Xu);

Abstract

Yarrowia lipolytica offers an ideal host for biosynthesis of high value natural products and oleochemicals through metabolic engineering despite being restricted to a limited number of selective markers, and counter-selection achieved primarily with *URA3*. In this work, we investigate *MET25*, a locus of sulfide housekeeping within the cell, to be exploited as a standard genetic marker. Divalent lead supplemented in media induces lead sulfide (PbS) aggregation in *MET25*-deficient cells such that deficient cells grow brown/black, and cells with functional copies of *MET25* grow white. Loss of *MET25* did not induce strict auxotrophic requirements for methionine in *Y. lipolytica*, indicating *MET25* deficiency could be rescued by alternative pathways. Plasmid and chromosomal-based complementation of *MET25* deficient cells on a double layer agar plate with nutrient gradients demonstrates delayed phenotype (white morphology) restoration, indicating post-transcriptional feedback regulation of methionine biosynthesis in this yeast. *MET25* deficient *Y. lipolytica* could be used as an efficient whole-cell lead sensor with detection limit as low as 10 ppm of lead in drinking water. We further tested whether *MET25* deficiency can be exploited to confer resistance to methyl-mercury through chemical neutralization and detoxification. Kinetic growth curves of wild type and *MET25*-deficient cells were obtained under varying concentrations of methylmercury and cellular toxicity to methyl mercury was calculated from the Hill equation. Our results indicate that methylmecury may not be used as the counter-selectable marker due to insignificant changes of growth fitness. This work demonstrates the utility of using *MET25* as a sensitive lead sensor and the challenges of using *MET25* as a counter-selectable genetic marker, as well as the complex regulation of methionine biosynthesis in *Y. lipolyitca*, which may shed lights for us to develop valuable biotechnological applications centering around the sulfur house-keeping metabolism of the nonconventional yeast.

Keywords: methionine biosynthesis, *Yarrowia lipolytica*, genetic marker, color associated screening, counter selection.

Running title: Sulfur house-keeping metabolism in oleaginous yeast

Introduction

With the limited number of auxotrophic markers in the oleaginous yeast *Yarrowia lipolytica*, establishing an additional counter selectable marker has potential to add significant value and versatility to the genetic toolbox with regards to engineering this host organism (Wong, Engel et al. 2017, Ma, Gu et al. 2020). *URA3* is the conventional selection marker used in a few yeast species including *Y. lipolytica* because it offers auxotrophic transformant screening as well as counterselection potential for marker removal, *via* 5'-FOA resistance (Fickers, Le Dall et al. 2003, Lv, Edwards et al. 2019). Great advancements in genome editing have been made in this host recently despite largely being restricted by this single genetic marker (Gao, Tong et al. 2016, Schwartz, Hussain et al. 2016, Gao, Tong et al. 2017, Schwartz, Shabbir-Hussain et al. 2017, Jang, Yu et al. 2018, Lv, Edwards et al. 2019). Counter selectivity is essential for performing iterative chromosomal gene integrations and ensuring that random integration of the selectable marker from the first round of genetic manipulations does not lead to false positives upon use of that marker in subsequent transformations (Lv, Edwards et al. 2019). The *LEU2* marker requires similar synthetically defined media, and an auxotrophic host strain (Le Dall, Nicaud et al. 1994, Larroude, Rossignol et al. 2018), but without any known methods offering counter selection. Hygromycin and the *hph* dominant marker give the advantages of antibiotic resistance selection (Holkenbrink, Dam et al. 2018, Wagner, Williams et al. 2018), largely decoupling cell death and fitness from essential nutrients, but includes disadvantages like dose-independent spontaneous resistance and still no counter selectivity (Otero and Gaillardin 1996). A mechanism in *S. cerevisiae* involving methionine provided counter selectivity, phenotypic indication and auxotrophy to methionine (Cost and Boeke 1996), and this had not yet been exploited in *Y. lipolytica.*

The *MET25* gene is found in *Y. lipolytica*, homologous to *MET15* found in *S. cerevisiae*, and various pathological species of *Candida*. *MET25* in *Y. lipolytica* encodes for O-acetyl homoserine sulfhydrylase (EC 2.5.1.49) with a length of 425 amino acids. This enzyme is found ubiquitously in various organisms (Yamagata 1976, Yamagata 1989), and is reported to be

responsible for catalyzing numerous reactions involved in sulfur metabolism. Some of these proposed reactions are listed in Table 1, almost all of which are involved in metabolism of amino acids containing sulfur. This enzyme will catalyze an acetyl transfer reaction between methanethiol and O-acetyl-L-homoserine to produce methionine and acetate (reaction 1). Reactions 2 indicate the use of hydrogen sulfide (H_2S) as a substrate in conjunction with other carbon backbone substrates. This indicates significant trans-activity with respect to various small carbon sources and the fixation/sequestration of hydrogen sulfide in yeast.

The naming of the MET25 protein is somewhat confusing, as this locus has been studied by many other groups, in various hosts. *MET25*, *MET15*, and *MET17* are essentially synonymous in KEGG databases or NCBI catalogues. Since the discovery of *MET15* as a phenotypic locus, this same marker has been reported with methyl-mercury resistance (Singh and Sherman 1975, Ono, Ishii et al. 1991), for example, a color associated counter selectable marker was reported in *S. cerevisiae* (Cost and Boeke 1996), and this genetic tool has become a standard auxotrophic marker in *S. cerevisiae* strain BY4741 (Baker Brachmann, Davies et al. 1998, Sadowski, Su et al. 2007). Similarly, *MET15* has been utilized in *C. albicans* as a positive/negative color associated selection marker (Viaene, Tiels et al. 2000). *MET25* as a name seemingly came along when it was found that the promoter for O-acetyl homoserine sulfhydrylase in *S. cerevisiae* was highly tunable to methionine concentration *(Mumberg, Muller et al. 1994)*. The *MET25* promoter is used as a standard genetic part due to its tight tunability to methionine concentration. Specifically, we characterized the function of the genetic sequence found by YALI0D25168g (of the GRYC database) in this work. There is no current report to establish the MET25 functionality in *Y. lipolytica.*

The recent development of genome-editing tools have made *Y. lipolytica* an ideal host for various applications, ranging from biofuel production (Xu, Qiao et al. 2016, Qiao, Wasylenko et al. 2017, Xu, Qiao et al. 2017), to natural product biosynthesis (Liu, Marsafari et al. 2019, Lv, Marsafari et al. 2019, Zhang, Zhang et al. 2019, Gu, Ma et al. 2020, Liu, Wang et al. 2020, Ma, Gu et al. 2020, Marsafari and Xu 2020) and commodity chemical manufacturing (Ledesma-Amaro, Dulermo et al. 2016, Cordova and Alper 2018, Gu, Ma et al. 2020). To further

expand the genetic toolbox and understand the complex regulation of sulfur metabolism, we hypothesized that *MET25* could be utilized as a counter selectable color-associated genetic marker in *Y. lipolytica* and the complementation of MET25 will restore the cell phenotype. In this report, we used both homologous recombination and episomally expressed CRISPR-Cas12/cpf1 nuclease to disrupt *MET25*. We characterized the phenotype of *MET25*-deficient cells under the colorogenic media (soluble lead acetate) or counter-selectable media (methyl mercury). With plasmid-based or chromosome-based complementation of *MET25*, we also validated whether the phenotype could be restored. Based on a double-layer slanted agar with gradients of methionine, we inferred the post-transcriptional feedback regulatory mechanism underlying methionine biosynthesis. The development of *MET25* may further expand our ability to enable *Y. lipolytica* as an oleaginous yeast for various biosensing, bioremediation, bioproduction and biomedical applications.

Results

Chromosomal disruption of MET25 *via* homologous recombination

We first attempted to disrupt *MET25* via the conventional homologous recombination methods using a *URA3* disruption cassette. A black phenotype was observed on 37.5% (3/8) colonies picked from the CSM-Ura plate and spotted onto MLA (modified lead agar). (Supplementary Figure 1). This did not guarantee a true homogeneous population of *ΔMET25* mutants due to the possibility of mixed colonies from the CSM-Ura plate. This mixed population was confirmed visually by serial dilution and spreading on another MLA (modified lead agar) plate, where white and black colonies can be observed (Fig. 1A). This colony isolation was repeated (Supplementary Figure 2.A) until a true homogenous population of black colonies was observed, (Supplementary Figure 2.B)

Results regarding methionine auxotrophic requirements vary from reports in other yeasts. Knocking out the *MET25* locus in *Y. lipolytica* did not produce a strict methionine

auxotroph as *MET15* does in *S. cerevisiae* (Cost and Boeke 1996). Similarly, knockout of the appropriate homologue in *C. albicans* did not create an auxotroph (Viaene, Tiels et al. 2000). In order to test whether *MET25* is a strict methionine auxotrophic marker, colonies derived from Po1f, Po1f Δ*Met25*, and Po1fΔ*Met25* with pYLXP'-*Met25* were spotted on various media to confirm *MET25* deficiency and *MET25* restoration (Figure 2, and Supplementary Figure 3-6). The double dropout media, CSM-Leu-Ura plates, was used as control for the three genetic variants to ensure the correct genotype (supplementary figure 5). CSM-Met plates demonstrated to have little to no effective difference, indicating the existence of a methionine rescue pathway or contributions from media when spotting the plates. To rule out the pre-culture media effect, the cells were washed with PBS buffer and plated again onto CSM-Met (Supplementary Figure 3). We observed less growth in *ΔMET25* mutants, indicating clear cellular burden imposed on *ΔMET25* cells, although it did not induce a strict requirement for methionine. Cystathionine beta-lyase, *METC*, (YALI0D00605g) was hypothesized as the potential rescue pathway. The hypothesis was that by inhibiting the critical intermediate reaction between converting cystathionine to methionine, a methionine auxotrophic strain may be observed. The double knockout Po1fΔ*Met25*Δ*MetC*, also grew (data not shown) on methionine deficient media (CSM-Met), albeit with a diminished growth rate. We concluded that cystathionine beta-lyase does not appear to be a critical enzyme in the methionine rescue pathway responsible for conferring growth to our host without methionine.

Genome-editing of *MET25 via* CRISPR-cas12/cpf1 nuclease

We also sought to disrupt *MET25 via* CRISPR-cas12/cpf1 in order to orthogonally demonstrate the same locus as a target for disruption with phenotypic indication. After transformation of Po1f with the dual expression plasmid pYLXP'-*AsCpf1-AsCrRNA-Met25*, colonies from CMS-Leu plates were then rescreened on MLA and grew for 72 hours for visible black sectoring to be observed in 1/16 samples. By the end of 7 days, 6 out of 16 sample had black sectors and after 14 days 11/16 had visible sectors (Figure 3). This indicates the genome-editing of *MET25* with CRISPR-Cpf1 depends on prolonged genome-targeting and cutting, as makes sense since the Cpf1 protein and associated RNA need time to be synthesized,

folded, and located properly in vivo for their individual roles to be completed together. Phenotypically indicative sectors were colony isolated and *Met25* was sequencing verified to contain an indel knockout*(Yang, Edwards et al. 2020)*. The *MET25* locus provides an easy target for testing gene disruption efficiency with a phenotypic indication. *MET2*(YALI0E00836g), and *MET6(*YALI0E12683g) were all independently targeted with the same plasmid based Cpf1 gene disruption platform with success in achieving phenotypic selection(Yang, Edwards et al. 2020).

Delayed phenotype restoration of *MET25* deficiency indicates orthogonal feedback regulation of methionine biosynthesis in *Y. lipolytica*

We next investigated whether we could restore the white colony phenotype by complementing *MET25* deficiency using either plasmid or chromosomal-based expression of *Met25*. Use of *MET25* alone in rich MLA media has proven difficult due to the lack of counter-selection pressure for negative transformants: almost all populations of transformants were black on the MLA plate, indicating either low transformation efficiency or negative transformants. To overcome this limitation, we next pursued a 2-step screening: we first screened the *LEU2* marker on CSM-leu plate to ensure expression of *MET25*, then the isolated colonies were replicated to MLA plate to validate phenotype restoration.

Episomal or chromosomal expression of *MET25* in *ΔMET25* cells proved difficult to restore the white colony phenotype, but the results of continued interest alluded to interesting regulation of methionine. Upon complementation with this *MET25* deficient host, the white phenotype was not observed initially (Fig. 1B). The cells grow in CSM-Leu, indicating the retention of the *LEU2* marker from the plasmid containing *MET25*. Re-streaking the colonies isolated from CSM-Leu also grew black on MLA, indicating no functional complementation of *MET25* from the plasmid or chromosomal-based *MET25* expression cassette, despite functional *LEU2* expression. After leaving the black transformant colonies in the incubator past 7 days, a white ring appeared radially surrounding a black core (Fig. 1B), as more generations grew. Colonies isolated from the white ring were re-streaked on MLA plates, demonstrating the similar patterns: a black core was surrounded by a white ring. MLA is rich media, and CSM-Leu/CSM-Met cannot stably contain the divalent lead without salting out so we cannot

perform this phenotypic assay in minimal media. Since genetic knockout was validated by sequencing, we hypothesized that media contributions of methionine were causing the effect. Results from the first CSM-Met assays (Supplementary Figure 3), preliminarily indicated an extremely sensitive feedback mechanism to inhibit methionine synthesis by methionine despite *MET25* being expressed by an orthogonal promoter.

This hypothesis was further validated with the double-layer, slanted agar plate assay with a gradient concentration of methionine (Figure 4). The increasing size of the white ring was accompanied with a decreasing methionine concentration (Fig. 4), in both the plasmid and the chromosome-based complementation of the *MET25* gene. This assay confirmed that methionine was negatively autoregulating the functional expression of the *MET25* gene. For example, the critical outer diameter of the white ring was observed to be inversely proportional to the local methionine concentration (Fig. 4). In order to ensure it was methionine diffusion, a slanted agar plate was poured with MLA on bottom and CSM-Met on top and no coloration was observed (Fig. 4), indicating that Pb^{2+} diffusion was not causing the change of fitness of the cell.

The white ring of the *MET25* complementation experiment suggests the methionine existing in the MLA media may produce feedback to inhibit the translation of *MET25* mRNA transcripts in *Y. lipolytica*, since it was orthogonally expressed via the *TEF2* promoter and *XPR2* terminator in our plasmid. The delayed phenotypic restoration in radially growing colonies indicated that there was sufficient amount of methionine inhibiting the expression of *MET25* in early growth stage, as a result, expression of *MET25* was not required, sulfur was not utilized, and the colonies remain black. At a later time when methionine was limited or depleted, expression of *MET25* was required, utilizing sulfur, and the new cells grew with their original white phenotype. It has been seen that there are multiple levels of regulation for *MET25* and methionine synthesizing pathways, including activating sequences of promoter regions, and post transcriptional interactions between methionine and the 5' region of the mRNA transcript(Thomas, Cherest et al. 1989). In our case, the timing of the phenotypic shift is affected by methionine concentrations when expressed under an orthogonal promoter (*TEF2*) and terminator (*XPR2*), whether plasmid or chromosomally expressed. Our results allude to

allosteric effects of methionine and Met25 the enzyme, co-repressor effects between methionine and an orthogonally expressed transcriptional factor, or post transcriptional activity between methionine and the *MET25* transcript.

MET25 deficient yeast as a whole cell senor to detect lead in potable water

Heavy metals in water have been linked with many diseases and have long been associated with neurodegenerative conditions in both kids and aged population. Since *MET25* deficiency leads to black pigmentation and form PbS precipitates, *MET25* deficient cells may be used as a whole-cell sensor to detect lead in potable waters. In order to gauge the applicability of this strain for microbially-based lead sensing purposes, the *ΔMET25* mutants were cultivated on MLA media containing 1000, 100, 10, and 0 mg/L (ppm), of soluble lead (II) nitrate, (Fig. 5). Yeast colonies and surrounding media were darkened in 100 ppm lead, by 24 hours, and significantly darker by 48 and 72 hours. Colonies gown on 10 ppm lead (II) MLA plates were visually darker after 72 hour's cultivation (Fig. 5). These results indicate a high level of sensitivity could be achieved by a simple, microbial-based lead bioassay, reaching the detection limits of 10ppm (Fig. 5). Further genetic engineering may be needed to tune the sensitivity and dynamic range of this whole cell microbial probe even further. If the local sulfide concentration can be increased, or sulfate-related transporter genes could be manipulated, this organism could provide a scalable and effective, low cost, non-electric whole microbe sensor for heavy metals.

Growth rates and counter-selection test toward methylmercury

We next attempted to determine the strength of the counter-selectivity toward methyl mercury in the *MET25* deficient strain. This specific growth rates for Po1f and Po1fΔ*Met25* were obtained by the slope of the linear regression of OD data versus time plotted on a logarithmic scale (equation No. 1). Then the specific growth rates were plotted against the level of methyl mercury to quantify the dose response relationship. Analyzing these specific growth rates in YPD at varying concentrations of methyl mercury in 96-well plates demonstrates a well fit with a Hill-type equation, governing the sigmoidal relationship between specific growth rate and methyl mercury concentration (Figure 6). The half inhibitory constants for Po1f and Po1fΔ*Met25* against methyl mercury were estimated at 0.746 μM and 1.383 μM respectively. As

237 expected, with the deletion of the *MET25* gene, the mutant cells become more resistant to
238 methyl mercury although by such a small margin, the practical applications (i.e. genetic
239 selection with a <0.5 μM window of counter selectivity) are difficult to achieve.

240 ## Discussion

241 Disruption of the *MET25* locus in *Y. lipolytica* via homologous recombination, or through
242 targeted indel knockouts, certainly induces the formation of brown/black colonies in the
243 presence of lead (II). The *ΔMET25* mutant generated visibly darker coloration to the naked eye
244 on media containing as low as 10 ppm lead. These findings alone indicate a potential for
245 biochemical engineers to develop a low cost, easy to use, microbial lead sensor for point of care
246 applications in regions with polluted water. This was not the objective at the start of this
247 experiment but the authors felt compelled to note this large dynamic range, and applicable
248 sensitivity to a common heavy metal, after just one deletion. Further genetic engineering of
249 microbial sulfur metabolism could increase lead detection sensitivity by increasing intracellular
250 sulfide availability through limiting other metabolic steps that consume sulfide. The formation
251 of lead (II) sulfide alludes to other possible sulfide and heavy metal chemistry, including the
252 formation of color distinct cadmium sulfide or cadmium selenide.

253 CRISPR-Cpf1/Cas12-mediated genome editing targeting the *MET25*, *MET2*, or *MET6* loci
254 was able to successfully induce black colony sectoring in Po1f, indicative of successful indel
255 mutation or gene knockout(Yang, Edwards et al. 2020). These loci *MET25*, *MET2*, and *MET6* all
256 provide similar behavior to target any of those genes for knockout, and a subsequent phenotypic
257 screening. Knocking out any one of these *MET* genes individually does not induce an
258 auxotrophic requirement for methionine, indicating that methionine can be biosynthesized via
259 alternative route. Cystathionine β -lyase, EC.4.4.1.13, or *METC*, was knocked out, along with
260 *MET25*, creating a double mutant which still was able to synthesize methionine to sustain
261 growth. There is a methionine-adenine salvage cycle reported in plants and bacteria(Sauter,
262 Moffatt et al. 2013), and we identified homologous proteins for the methionine salvage pathway
263 in *Y. lipolytica*, pointing there for future genetic engineering targets to engineer a strict
264 methionine auxotrophic strain. With the ubiquitous cellular requirement for methionine,

considering it is also the start codon, it is likely advantageous for being redundant in pathways for housekeeping of enzymes responsible for methionine biosynthesis.

The chromosomal deletion of *MET25* induced resistance to the toxic chemical methyl-mercury and a Hill type relationship was demonstrated between the specific growth rate and the methyl-mercury concentration. The difference in half inhibitory constant (IC_{50}) between the wildtype and mutant was about 0.6 μM, and this represents a challenge in exploiting this small window for counter selection. Since growth curves were in liquid media, those numbers were not helpful in determining a useful screening concentration of methyl-mercury on agar plates, and plate screening proved continuously difficult. Counter selection and phenotypic screening cannot be combined easily as the same intracellular sulfide affording a slight resistance to methyl mercury, is the same sulfide covalently reacting with lead to form a PbS black precipitate. If sulfide is utilized for color indication, it cannot also save the cells by neutralizing methyl mercury. Phenotypic screening and dropout media also could not be done together due to lead salts forming with nutrients in minimal media.

Most interestingly, even when *MET25* is expressed orthogonally via an independent promoter and terminator set (p*TEF2* and *XPR2*), there is still negative autoregulation of *MET25* activity due to local methionine availability. Further work should investigate differential gene expression under these conditions, and quest for the transcriptional factors (TFs) involved in this regulation, as well as perform calorimetric and energetic binding assay between the TFs, methionine, the *MET25* template DNA, and the *MET25* mRNA transcript. This may help us uncover a potentially novel feedback regulation mechanism in methionine biosynthesis apart from the commercialized *MET25* promoter. Considering the phylogenic age of the amino acid located at each and every start codon, there may be a robust and ubiquitous method of regulation like the tryptophan attenuation loop, or this could be a complex interaction network of transcription factors as is often not completely understood in eukaryotic signaling networks. Further investigation into the mechanism of feedback for methionine and *MET25, like quantitative RT-PCR to investigate the expression of critical genes in the pathway,* should be pursued for regulatory discovery. Further work should also standardize the phenotypic screening

methods with the sulfur-housekeeping marker in *Y. lipolytica*, due to the very sensitive operating range of the methylmecury as a toxic selection agent.

Conclusions

The *MET25* marker in *Y. lipolytica* can offer phenotypic screening of transformants quite easily on rich media supplemented with lead(II)acetate. Positive screening with *MET25* and solely lead has proven difficult as there is no negative selection pressure to limit growth of negative transformants and a methionine auxotrophic strain was not observed either. To overcome this limitation, counterselection is narrowly achieved via growth on rich media containing methyl-mercury. Methyl-mercury is toxic, and could be detoxified by sulfide buildup in the *ΔMET25* cells, due to the formation of mercuric sulfide and ethanol conferring toxic resistance to methyl mercury. The counter-selection window, at barely 0.5 micromolar in liquid media, makes this technique difficult to practically achieve. Both positive/negative screening, and counter selection can be done in rich media, although not in a single assay/plate due to synergistic effects of sulfide on both the mechanism of toxic resistance and the mechanism of phenotypic distinction.

MET25 in our system was overexpressed via the *TEF2* promoter and *XPR2* terminator, but still, methionine-based autoregulation of this gene, observed in the slanted plate agar test, increased difficulty in consistent results with this strain. Counter selection was barely achieved and the narrow window of counter selectivity makes this technique difficult. Combined with the potential health hazards associated with mercury reagents and bioassays which use them, methyl-mercury selection is less than ideal. Further genetic engineering should work to build a methionine auxotroph, which would alleviate the necessity for methyl mercury counter selection, and should focus on increasing the rate and magnitude of this sulfide buildup to further leverage phenotypic and genetic selection traits. Utilizing these methods in rich media has potential to increase the rate at which transformants grow and are screened, which may significantly decrease the time spent on engineering this host. This selectable marker also facilitates better understanding of cellular regulation because of the visual indications of genetic events indicated by sectoring or delayed phenotype expression.

Materials and methods

Plasmids, strains and media

Y. lipolytica Po1f (ATCC MYA-2613, MATA ura3-302 leu2-270 xpr2-322 axp2-deltaNU49 XPR2:SUC2) was used as the host strain. *Escherichia coli* NEB5α was used for plasmid construction and proliferation. The YaliBrick plasmid pYLXP' was used as the backbone to construct other plasmids (Wong, Engel et al. 2017). LB broth or agar plates containing ampicillin (100 mg/L) was routinely used for *E. coli* cultivation. YPD media consisting of 10 g/L yeast extract, 20 g/L peptone and 20 g/L glucose and complete synthetic media (CSM) omitting proper amino acids were used for yeast cultivation and transformation. MLA plates containing 3 g/L peptone, 5 g/L yeast extract, 0.2 g/L ammonium sulfate, 40 g/L glucose, 1 g/L lead nitrate and 20 g/L agar were used for visual selection of *met25* mutants. Lead nitrate was filter sterilized and added to autoclaved mixture of other components after cool down.

Met25 Disruption via Homologous Recombination

All primers used in this work were listed in supplementary table 1. To construct a cassette for the deletion of *MET25*, primers met25upfw and met25uprv were used to PCR amplify an 800 bp fragment immediately upstream from the start codon of *MET25* using genomic Po1f DNA as template. This fragment was size verified via gel electrophoresis and purified using ZYMO Clean and Concentrator kits. Another 800 bp fragment immediately downstream from the stop codon was obtained using primers met25dwfw and met25dwrv. The gene *ylUra3* had previously been functionally cloned in our lab, into the plasmid pYLXP', to create pYLXP'-*ylUra3*. That plasmid was linearized with *Sal*I and gel purified. The downstream 800 bp fragment was cloned into the *Sal*I digested vector backbone to yield pYLXP'-*ylUra3*-Met25DW, via Gibson assembly, transformed into *E. coli* and screened on LB agar plates.

Colonies were verified via colony PCR using xpr2_fw and met25dwrv. Positive colonies were inoculated into LB media containing ampicillin for overnight culture. Plasmid was purified using ZYMO Miniprep kits and sanger sequenced. The upstream 800 bp fragment was cloned

into pYLXP'-*ylUra3*-Met25DW digested with *Cla*I to yield pYLXP'-*ylUra3*-Met25. The primers tef-rv and met25upfw were used for colony PCR to screen colonies for a 900 bp fragment. The sequencing-verified pYLXP'-*ylUra3-Met25* was used to PCR amplify a deletion cassette of *MET25* using primers met25cassfw and met25cassrv.

The *MET25* knockout cassette was transformed into wild type Po1f strain using hydroxyurea-based protocol to enhance homologous recombination(Tsakraklides, Brevnova et al. 2015),(Jang, Yu et al. 2018). Transformants were plated onto CSM-Ura plates. These preliminarily positive transformants were diluted into 10 µL sterile water and then used for selective media assays. These transformants were screened on MLA plates (Supplementary figure 1) and colonies which turned dark in color were picked to inoculate in CSM-Ura liquid media. That liquid culture was diluted and streaked on MLA to perform colony isolation. A single black colony was picked and inoculated into CSM-Ura liquid media, incubated 24 hrs, diluted, and re-plated to ensure that a true homogenous population of *ΔMET25* mutants was obtained. (Supplementary Figure 2)

Plasmid and Chromosomal Complementation of Met25

MET25 was PCR amplified out of genomic Po1f DNA using the primers met25fw and met25rv and cloned into vector pYLXP' to yield pYLXP'-Met25. This plasmid was transformed into *ΔMET25* cells and plated onto CSM-Leu plates. Positive transformant were plated onto various selective medias (Supplementary Figures 3 to 6) for comparison of growth behavior and *MET25* expression in the wildtype Po1f, mutant Po1f+*ylUra3-Met25*, and mutant containing plasmid Po1f+*ylUra3-Met25* and pYLXP'-*Met25*. A graphic summarizing these plates can be observed in figure 2.

Growth assay in CSM-Met selective media were performed in order to test if the *MET25* knockout could confer auxotrophic requirements for methionine. Results were negative, as po1f-*ylUra3-ΔMET25* grew on CSM-Met plates when spotted from CSM-Ura liquid culture. The experiment was repeated to see if methionine in the liquid media was enabling growth. In this case cell cultures of each sample were grown for 2 days in appropriate selective media and centrifuged at 1800xg for 10 minutes to pellet cells. The supernatant was discarded, the pellet

was resuspended in PBS and this entire wash was repeated to ensure no nutrient from the media is transferred with the cells that inoculate the selective media plates. These two plates are observed in Supplemental Figure 3.

To construct a strain with chromosomally integrated expression cassette of *MET25*, pYLXP'-*Met25* was linearized with NotI, a restriction site flanked by a chromosomal landing pad of complementary bases(Wong, Engel et al. 2017). The linearized plasmid was transformed into mutant cells and plated onto CSM-Leu plates. Colonies were inoculated into YPD liquid media for 72 hours and spread onto CSM-Leu plates. Single colonies from this plate were taken as chromosomal integrations of the plasmid.

Met25 Disruption via CRISPR/Cpf1 Mediated Indel Mutation

In order to gauge the applicability of CRISPR/Cpf1 mediated, transient gene disruption of a phenotypic locus, and to orthogonally demonstrate the responsibility of the *MET25* gene in the lead(II) sulfide producing cells, a single plasmid was created containing a functional copy of *AsCpf1* and *AsCrRNA_Met25*. *AsCrRNA_Met25* is the gene enconding the guide RNA created analogous to the gRNA of the *CAN1* design(Wong, Engel et al. 2017). The construction of CRISPR-Cas12 plasmids used to knockout *MET25*, *MET2*, and *MET6* can be found in literature(Wong, Engel et al. 2017, Yang, Edwards et al. 2020). pYLXP'-*AsCpf1-AsCrRNA-Met25* was transformed into Po1f and plated onto CSM-Leu, incubated for 72 hours, and colonies were screened on MLA plates by picking single colonies into 10 μL sterile water, and spotting 3 μL on CSM-Leu, and 3 μL on MLA. These two plates were incubated for 48-72 hours (Supplementary Figure 4).

MetC, and Met25 Double Knockout

A gene disruption cassette utilizing *ylUra3* marker was created and employed, using identical techniques as described in section 2.1, this time with 800 bp homologous arms designed to initiate homologous recombination in the *METC* (YALI0D00605g) locus. Colony PCR verification was performed using MetCupchk and tef-rv, as well as MetCdwnchk and xpr2-fw, for a 900 and 1000 bp fragment indicating successful integration, respectively. Positive

colonies from colony PCR verification are now grown in CSM-Ura and designated as Po1f+*ylUra3-MetC*.

pYLXP'-*AsCpf1-AsCrRNA-Met25* was then transformed into Po1f+*ylUra3-MetC*. Transformants were grown on CSM-Leu for 72 hrs. Colonies were then picked, resuspended in 10 µL sterile water, and plated onto MLA plates. Once black sectoring was observed, this colony was chosen, diluted and spread onto MLA to isolate a single, black colony. This took three rounds of colony resuspension, dilution, plating, and isolation, before a homogeneous population was observed. This transformant was designated Po1fΔ*Met25+ylUra3-MetC*. This strain was assayed for an auxotrophic methionine requirement on CSM-Met plates.

Selective Media and Differential Growth Test

All selective media agar plates use 2% agar. Dropout media CSM-Leu and CSM-Ura plates were used to selectively screen positive transformants. CSM-Met and CSM-Leu-Ura were employed to observe burden associated with different autotrophies, and to verify plasmid holding mutants respectively. Modified lead agar, MLA, plates were made with 1 g/L lead(II) nitrate(Van Leeuwen and Gottschling 2002), (Cost and Boeke 1996) YPD plates containing 4µM and 8µM methylmercury were used to investigate counter-selectivity. In order to establish a gradient of nutrients, agar plates were partially filled with CSM-Met, and the plates were tilted and allowed to cool such that the gel set diagonally. The plate was then poured the rest of the way with MLA media, ensuring to cover the minimal media entirely, and allowed to set again. This was repeated with MLA media on bottom and CSM-Met on top too. The results of the media assays with an established nutrient gradient are found in Figure 4. The authors apologize for resolution lost in attempt to demonstrate many pictures at once. Higher resolution images of the original plates are available in the supplementary information.

In order to more quantitatively observe response and gauge the utility of methylmercury as a counter-selection agent, specifically in Y. lipolytica, growth rates were measured in liquid media at varying concentrations of the methyl mercury. Po1f and Po1f+ylUra3-Met25 were inoculated in YPD and cultured for 24 hours. OD600 was normalized at 0.15 in the wells, and measurements were taken on a 96-well microwell-plate reader, during incubation at 30 degrees

C with full shaking. OD was measured every 10 minutes for 8 hours. These readings were fit linearly on a logarithmic scale and the slope recorded as the specific growth rate. The specific growth rate was normalized with the maximum value to determine the relative growth rate labeled in percent of the maximum specific growth rate. These specific growth rates were plotted at various concentrations to visually establish a relationship for Po1f and Po1fΔMet25. Specific growth rates can be estimated by equation No. 1; and the inhibitory constant could be determined by the following Hill type equation (equation No. 2).

$$\mu = \frac{d\ln(OD)}{dt} \quad \text{Equation.1}$$

$$\mu = A_1 + \frac{(A_2 - A_1) * X^n}{K^n + X^n} \quad \text{Equation.2}$$

Acknowledgements

This work was funded by the Bill & Melinda Gates Foundation under grant no. OPP1188443. as well as the National Science Foundation (Award Number 1805139). The authors also acknowledge the support from University of Maryland, Baltimore County, and the Department of Chemical, Biochemical, and Environmental Engineering.

Author contributions

PX conceived and designed the topic. HE and ZY performed genetic engineering. HE wrote the manuscript. PX and ZY revised the manuscript.

Conflicts of interests

There are no conflicts of interest to report in this work.

References

Baker Brachmann, C., A. Davies, G. J. Cost, E. Caputo, J. Li, P. Hieter and J. D. Boeke (1998). "Designer deletion strains derived from Saccharomyces cerevisiae S288C: A useful set of strains and plasmids for PCR-mediated gene disruption and other applications." Yeast **14**(2): 115-132.

Cordova, L. T. and H. S. Alper (2018). "Production of α-linolenic acid in Yarrowia lipolytica using low-temperature fermentation." Applied Microbiology and Biotechnology **102**(20): 8809-8816.

Cost, G. J. and J. D. Boeke (1996). "A useful colony colour phenotype associated with the yeast selectable/counter-selectable marker MET15." Yeast **12**(10): 939-941.

Fickers, P., M. T. Le Dall, C. Gaillardin, P. Thonart and J. M. Nicaud (2003). "New disruption cassettes for rapid gene disruption and marker rescue in the yeast Yarrowia lipolytica." Journal of Microbiological Methods **55**(3): 727-737.

Gao, S., Y. Tong, Z. Wen, L. Zhu, M. Ge, D. Chen, Y. Jiang and S. Yang (2016). "Multiplex gene editing of the Yarrowia lipolytica genome using the CRISPR-Cas9 system." Journal of Industrial Microbiology & Biotechnology **43**(8): 1085-1093.

Gao, S., Y. Tong, L. Zhu, M. Ge, Y. Zhang, D. Chen, Y. Jiang and S. Yang (2017). "Iterative integration of multiple-copy pathway genes in Yarrowia lipolytica for heterologous beta-carotene production." Metab Eng **41**.

Gu, Y., J. Ma, Y. Zhu, X. Ding and P. Xu (2020). "Engineering Yarrowia lipolytica as a Chassis for De Novo Synthesis of Five Aromatic-Derived Natural Products and Chemicals." ACS Synthetic Biology **9**(8): 2096-2106.

Gu, Y., J. Ma, Y. Zhu and P. Xu (2020). "Refactoring Ehrlich Pathway for High-Yield 2-Phenylethanol Production in Yarrowia lipolytica." ACS Synthetic Biology **9**(3): 623-633.

Holkenbrink, C., M. I. Dam, K. R. Kildegaard, J. Beder, J. Dahlin, D. Doménech Belda and I. Borodina (2018). "EasyCloneYALI: CRISPR/Cas9-Based Synthetic Toolbox for Engineering of the Yeast Yarrowia lipolytica." Biotechnology Journal **13**(9): 1700543.

Jang, I.-S., B. J. Yu, J. Y. Jang, J. Jegal and J. Y. Lee (2018). "Improving the efficiency of

homologous recombination by chemical and biological approaches in Yarrowia lipolytica." PLOS ONE **13**(3): e0194954.

Larroude, M., T. Rossignol, J. M. Nicaud and R. Ledesma-Amaro (2018). "Synthetic biology tools for engineering Yarrowia lipolytica." Biotechnology Advances **36**(8): 2150-2164.

Le Dall, M. T., J. M. Nicaud and C. Gaillardin (1994). "Multiple-copy integration in the yeast Yarrowia lipolytica." Curr Genet **26**(1): 38-44.

Ledesma-Amaro, R., R. Dulermo, X. Niehus and J.-M. Nicaud (2016). "Combining metabolic engineering and process optimization to improve production and secretion of fatty acids." Metabolic Engineering **38**: 38-46.

Liu, H., M. Marsafari, F. Wang, L. Deng and P. Xu (2019). "Engineering acetyl-CoA metabolic shortcut for eco-friendly production of polyketides triacetic acid lactone in Yarrowia lipolytica." Metabolic Engineering **56**: 60-68.

Liu, H., F. Wang, L. Deng and P. Xu (2020). "Genetic and bioprocess engineering to improve squalene production in Yarrowia lipolytica." Bioresource Technology **317**: 123991.

Lv, Y., H. Edwards, J. Zhou and P. Xu (2019). "Combining 26s rDNA and the Cre-loxP System for Iterative Gene Integration and Efficient Marker Curation in Yarrowia lipolytica." ACS Synthetic Biology **8**(3): 568-576.

Lv, Y., M. Marsafari, M. Koffas, J. Zhou and P. Xu (2019). "Optimizing Oleaginous Yeast Cell Factories for Flavonoids and Hydroxylated Flavonoids Biosynthesis." ACS Synthetic Biology.

Ma, J., Y. Gu, M. Marsafari and P. Xu (2020). "Synthetic biology, systems biology, and metabolic engineering of Yarrowia lipolytica toward a sustainable biorefinery platform." Journal of Industrial Microbiology & Biotechnology.

Ma, J., Y. Gu and P. Xu (2020). "A roadmap to engineering antiviral natural products synthesis in microbes." Current Opinion in Biotechnology **66**: 140-149.

Marsafari, M. and P. Xu (2020). "Debottlenecking mevalonate pathway for antimalarial drug precursor amorphadiene biosynthesis in Yarrowia lipolytica." Metabolic Engineering Communications **10**: e00121.

508 Mumberg, D., R. Muller and M. Funk (1994). "Regulatable promoters of Saccharomyces
509 cerevisiae: comparison of transcriptional activity and their use for heterologous
510 expression." Nucleic Acids Research **22**(25): 5767-5768.
511 Ono, B., N. Ishii, S. Fujino and I. Aoyama (1991). "Role of hydrosulfide ions (HS-) in
512 methylmercury resistance in Saccharomyces cerevisiae." Applied and environmental
513 microbiology **57**(11): 3183-3186.
514 Otero, R. C. and C. Gaillardin (1996). "Efficient selection of hygromycin-B-resistant Yarrowia
515 lipolytica transformants." Applied Microbiology and Biotechnology **46**(2): 143-148.
516 Qiao, K., T. M. Wasylenko, K. Zhou, P. Xu and G. Stephanopoulos (2017). "Lipid production in
517 Yarrowia lipolytica is maximized by engineering cytosolic redox metabolism." Nat
518 Biotechnol **35**(2): 173-177.
519 Sadowski, I., T.-C. Su and J. Parent (2007). "Disintegrator vectors for single-copy yeast
520 chromosomal integration." Yeast **24**(5): 447-455.
521 Sauter, M., B. Moffatt, Maye C. Saechao, R. Hell and M. Wirtz (2013). "Methionine salvage and
522 S-adenosylmethionine: essential links between sulfur, ethylene and polyamine
523 biosynthesis." Biochemical Journal **451**(2): 145.
524 Schwartz, C., M. Shabbir-Hussain, K. Frogue, M. Blenner and I. Wheeldon (2017).
525 "Standardized Markerless Gene Integration for Pathway Engineering in Yarrowia
526 lipolytica." ACS Synthetic Biology **6**(3): 402-409.
527 Schwartz, C. M., M. S. Hussain, M. Blenner and I. Wheeldon (2016). "Synthetic RNA
528 polymerase III promoters facilitate high-efficiency CRISPR-Cas9-mediated genome editing
529 in Yarrowialipolytica." ACS Synth Biol **5**.
530 Singh, A. and F. Sherman (1975). "GENETIC AND PHYSIOLOGICAL
531 CHARACTERIZATION OF met15 MUTANTS OF
532 SACCHAROMYCES CEREVISIAE: A SELECTIVE SYSTEM FOR
533 FORWARD AND REVERSE MUTATIONS." Genetics **81**(1): 75.
534 Thomas, D., H. Cherest and Y. Surdin-Kerjan (1989). "Elements involved in
535 S-adenosylmethionine-mediated regulation of the Saccharomyces cerevisiae MET25 gene."

Molecular and cellular biology **9**(8): 3292-3298.

Tsakraklides, V., E. Brevnova, G. Stephanopoulos and A. J. Shaw (2015). "Improved Gene Targeting through Cell Cycle Synchronization." PLOS ONE **10**(7): e0133434.

Van Leeuwen, F. and D. E. Gottschling (2002). Assays for gene silencing in yeast. Methods in Enzymology. C. Guthrie and G. R. Fink, Academic Press. **350:** 165-186.

Viaene, J., P. Tiels, M. Logghe, S. Dewaele, W. Martinet and R. Contreras (2000). "MET15 as a visual selection marker for Candida albicans." Yeast **16**(13): 1205-1215.

Wagner, J. M., E. V. Williams and H. S. Alper (2018). "Developing a piggyBac Transposon System and Compatible Selection Markers for Insertional Mutagenesis and Genome Engineering in Yarrowia lipolytica." Biotechnology Journal **13**(5): 1800022.

Wong, L., J. Engel, E. Jin, B. Holdridge and P. Xu (2017) "YaliBricks, a versatile genetic toolkit for streamlined and rapid pathway engineering in Yarrowia lipolytica." Metabolic engineering communications **5**, 68-77 DOI: 10.1016/j.meteno.2017.09.001.

Wong, L., J. Engel, E. Jin, B. Holdridge and P. Xu (2017). "YaliBricks, a versatile genetic toolkit for streamlined and rapid pathway engineering in Yarrowia lipolytica." Metabolic Engineering Communications **5**(Supplement C): 68-77.

Xu, P., K. Qiao, W. S. Ahn and G. Stephanopoulos (2016). "Engineering Yarrowia lipolytica as a platform for synthesis of drop-in transportation fuels and oleochemicals." Proceedings of the National Academy of Sciences **113**(39): 10848-10853.

Xu, P., K. Qiao and G. Stephanopoulos (2017). "Engineering oxidative stress defense pathways to build a robust lipid production platform in Yarrowia lipolytica." Biotechnol Bioeng **114**(7): 1521-1530.

Yamagata, S. (1976). "O-Acetylserine and O-acetylhomoserine sulfhydrylase of yeast. Subunit structure." J Biochem **80**(4): 787-797.

Yamagata, S. (1989). "Roles of O-acetyl-l-homoserine sulfhydrylases in microorganisms." Biochimie **71**(11): 1125-1143.

Yang, Z., H. Edwards and P. Xu (2020). "CRISPR-Cas12a/Cpf1-assisted precise, efficient and multiplexed genome-editing in Yarrowia lipolytica." Metabolic Engineering

564 Communications **10**: e00112.

565 Zhang, R., Y. Zhang, Y. Wang, M. Yao, J. Zhang, H. Liu, X. Zhou, W. Xiao and Y. Yuan (2019).

566 "Pregnenolone Overproduction in Yarrowia lipolytica by Integrative Components Pairing of

567 the Cytochrome P450scc System." ACS Synthetic Biology.

568

569

Tables

Table 1. Short list of proposed reactions catalyzed by O-Acetylhomoserine aminocarboxypropyltransferase. Reactions are found linked to EC 2.5.1.49 *via* KEGG database, and chemical reactions were drawn with ChemDoodle.

Reactions	Proposed reactions catalyzed by O-Acetylhomoserine aminocarboxypropyl transferase (EC 2.5.1.49).
1	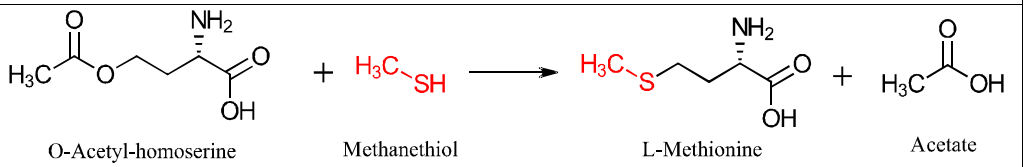
2	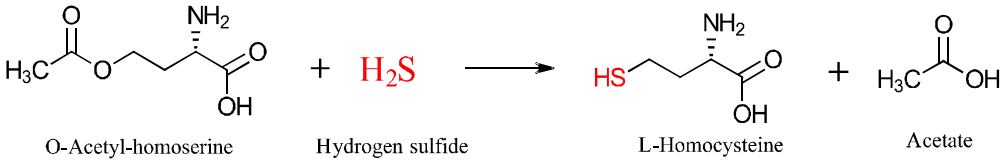

Figures

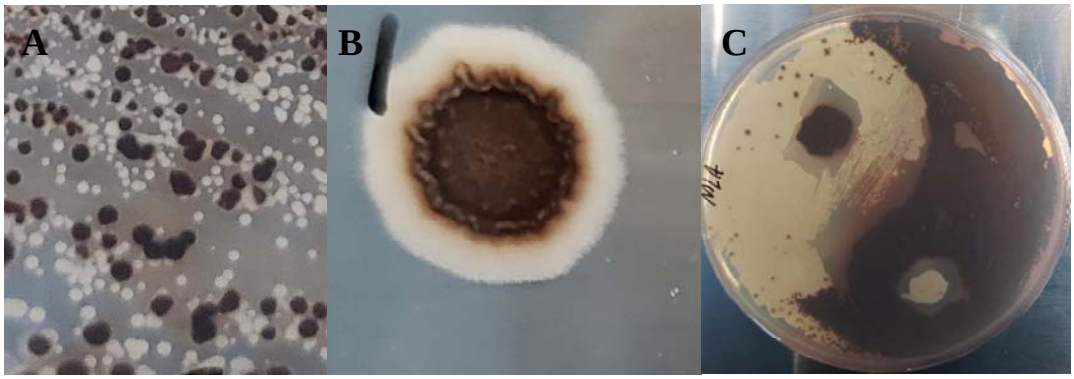

Fig. 1 Visibly formed black colony of MET25 deficient cell

Phenotypic separation of white and black colonies after *MET25* deletion (A). Plasmid-complementation of *MET25* in the *MET25*-deficient cell leads to the formation of a radially distributed white ring (B). Yin-Yang art (C) of wild type (white colony) and *MET25* deficient cells (black colony) on MLA plate.

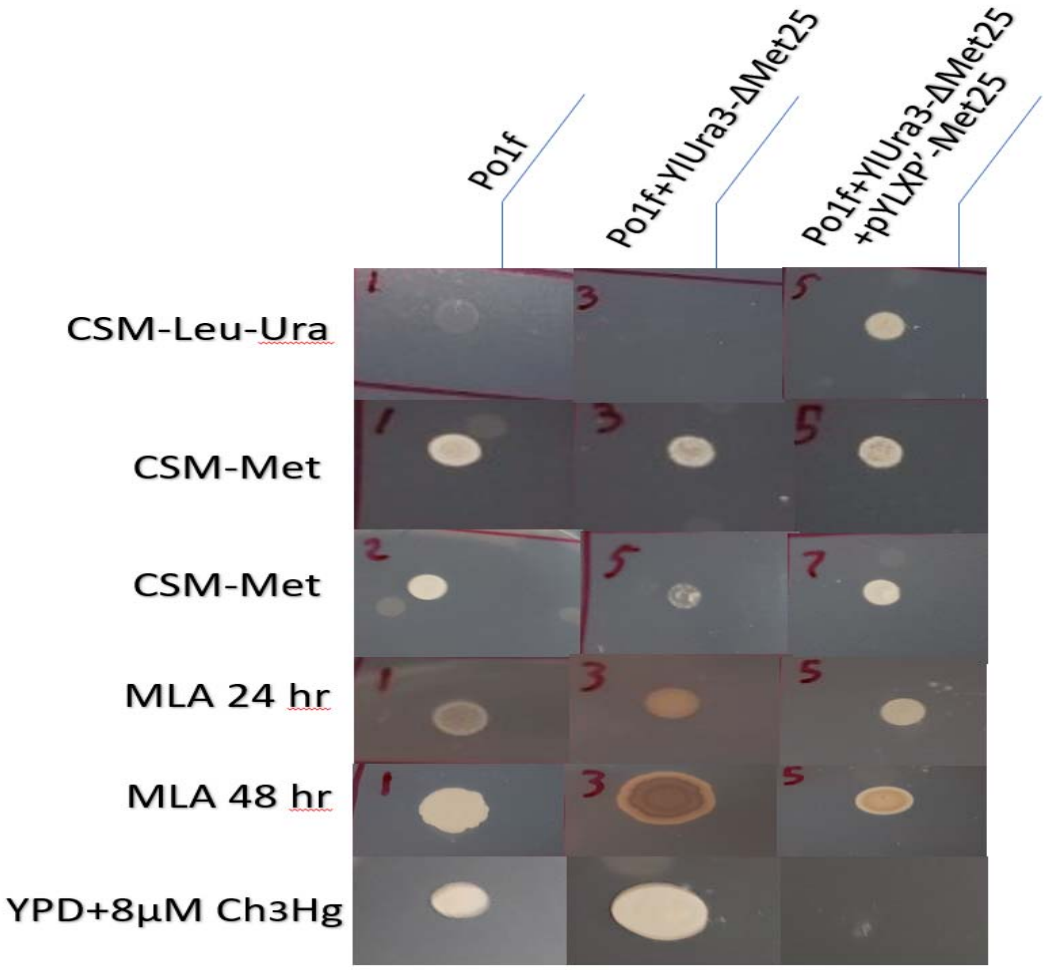

587

588 **Fig. 2. Collection of Selection Tests of MET25 deficient cell**

589 This image contains the result various selective media assays. The columns left to right
590 represent wildtype, mutant, and mutant containing restorative plasmid. The first row contains all
591 strains growing on CSM-Leu-Ura. The second and third row contain all strains growing on
592 CSM-Met, without and with cell washing, respectively. The fourth and fifth row demonstrates
593 all strains growing on MLA, at 24 and 48 hours, respectively. The strains in the sixth row were
594 grown on rich media containing 8mM methyl mercury. (The authors apologize for resolution
595 lost in an attempt to demonstrate many pictures at once. Higher resolution images of the original
596 plates are available in the supplementary information.)

597

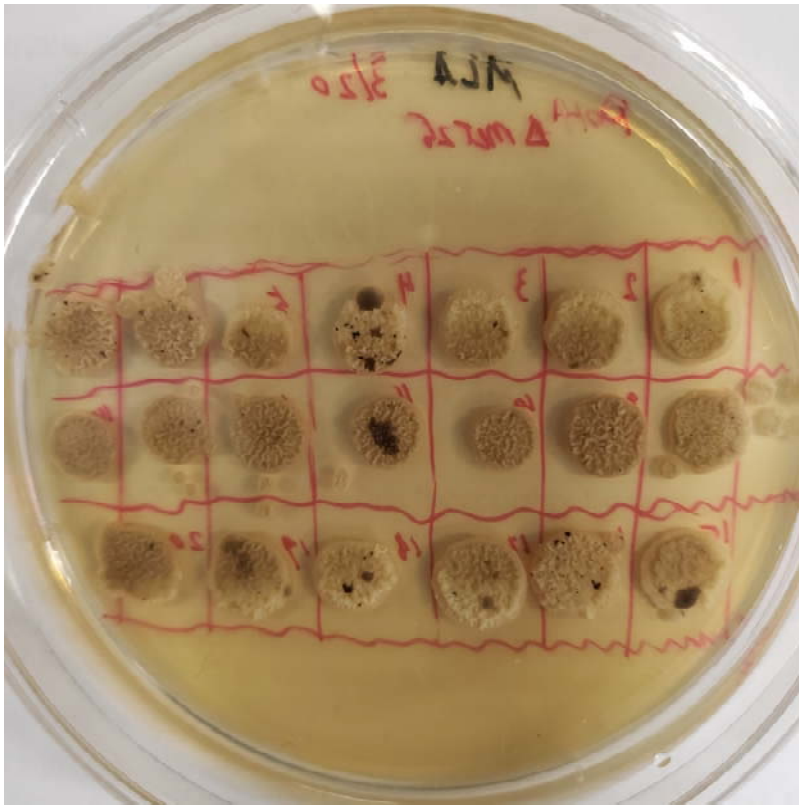

Fig. 3. Visible Sectoring After Transient Disruption of MET25 via CRISPR-Cas12 and Targeted crRNA

Colonies from a successful transformation of Po1f with pYLXP'-AsCpf1-AsCrRNA-Met25 on CSM-Leu, subsequently spotted onto MLA. Performing colony isolation on any black sector results in successful indel knockout of MET25.

606

607

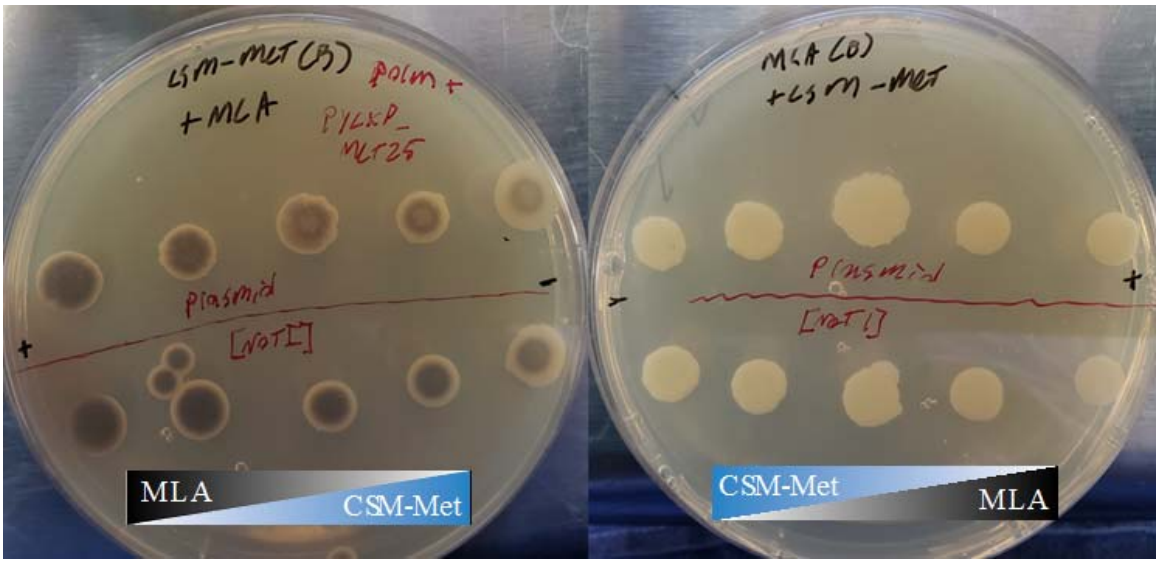

608

609 **Fig. 4. Dual-Media Slanted Agar Plates to detect MET25 phenotype restoration**

610 On the left panel, CSM-Met on bottom, MLA on top, decreasing methionine availability from
611 left to right. Phenotype restoration (white morphology) was observed to be increased with
612 decreasing methionine availability, indicating the presence of methionine inhibits the expression
613 of MET25 gene. On the right panel, MLA on bottom, CMS-Met on top, increasing methionine
614 availability from left to right. All tested colonies remained white, indicating there is no lead
615 diffusion from the bottom layer to the upper layer. Colonies with plasmid-based MET25
616 complementation are above the red equator line, colonies with chromosomally integrated
617 MET25 (*via Not*1 linearization) are below the red equator line.

618

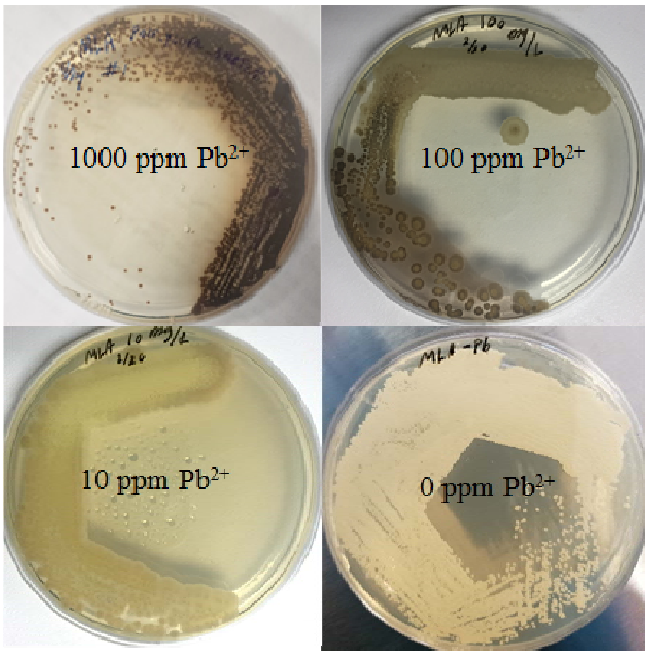

Fig. 5. **Phenotypic response of MET25 deficient strain to lead concentration ranging from 0 to 1000 ppm.**

MET25 deficient cells acting as biological probes for lead on MLA plates containing lead ranging from 0 ppm to 1000 ppm.

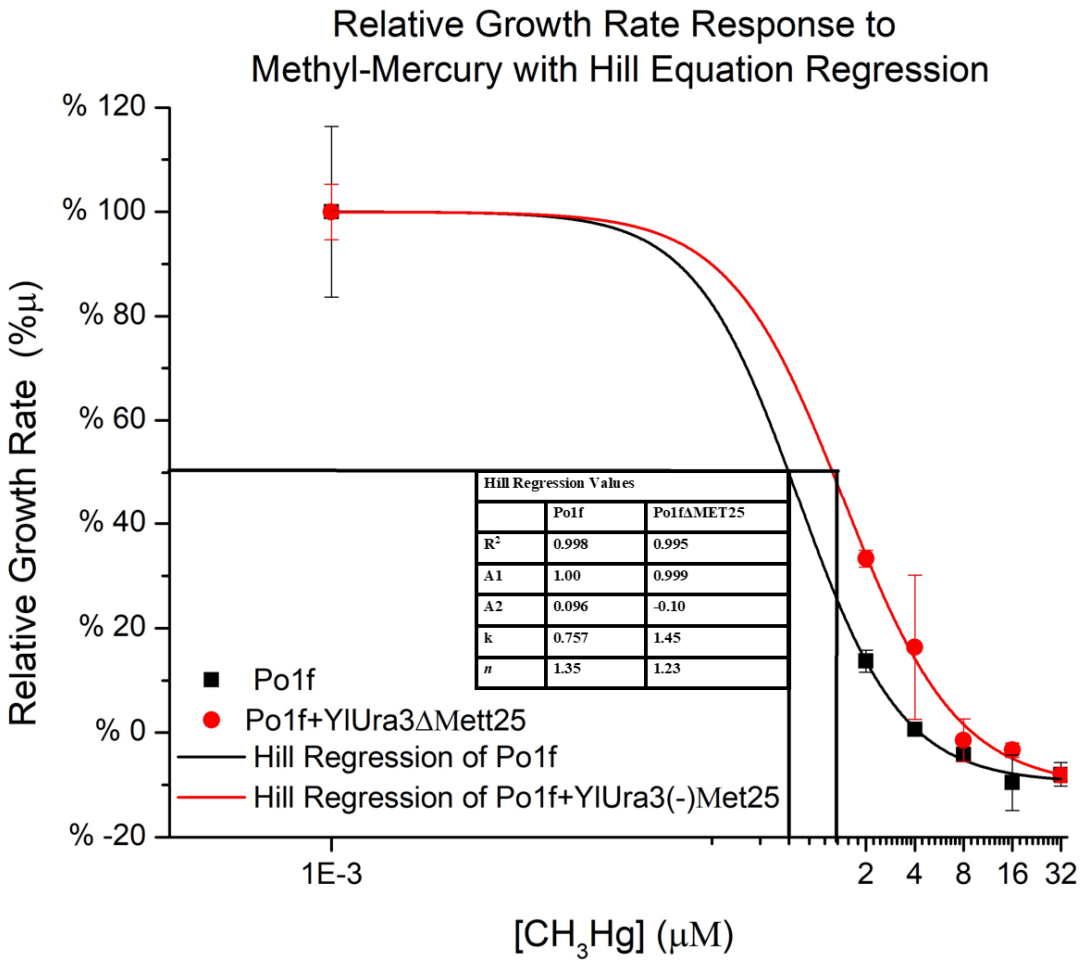

Fig. 6. <u>Relative Growth Rate Response to Methyl-Mercury</u>

Relative specific growth rate in the presence of methyl mercury is observed to correlate strongly with a Hill type equation. Points indicate biological triplicates where the lines represent regression curves. Black graphics indicate wildtype and red indicate mutants lacking *MET25*.